J. Fluid Mech. (1990), *vol.* 219, *pp.* 571–584
Printed in Great Britain

Natural-convection boundary-layer flow over a heated plate with arbitrary inclination

By A. UMEMURA AND C. K. LAW
Department of Mechanical and Aerospace Engineering, Princeton University, Princeton, NJ 08544, USA

(Received 10 April 1989 and in revised form 10 March 1990)

The natural-convection boundary-layer flow over a semi-infinite heated plate of arbitrary inclination is studied by first identifying a set of combined boundary-layer variables and then casting the governing equations into a universal form. The generalized problem yields the existing similarity solutions for the limiting cases of horizontal and vertical plates, and describes the gradual transition of the flow pattern between these two limits at distances from the leading edge which depend on the inclination angle. Near the leading edge the buoyancy force acting normal to the plate causes an 'impulsive' driving force to the fluid motion along the plate, while the 'regular' driving force exerted by the tangential buoyancy force becomes dominating downstream. Both the exact and the locally-similar solutions are obtained and are found to agree well with each other.

1. Introduction

For natural-convection boundary-layer flow over a heated flat plate, similarity solutions exist (Ostrach 1953; Stewartson 1958; Gill, Zeh & Del-Casel 1965) for the limiting situations of vertical ($\alpha = \frac{1}{2}\pi$) and horizontal ($\alpha = 0$) inclinations, where α is the angle of inclination of the plate to the horizontal plane. For a plate with arbitrary inclination except for very small values of α, most of the existing analyses have simply adopted the similarity solution for the vertical case, with the buoyant force being the component of the body force g along the plate. The reasoning being the anticipated dominance of the body force component along the plate as compared to that normal to the plate.

There are certain aspects which either are fundamentally unsatisfactory or require clarification with the above approximation. The first is its inability to describe flows with small α and the associated transition to large α behaviours. In fact the proper parametric grouping through which 'small' and 'large' α can be defined has not been identified. Furthermore, since the similarity solutions scale with $x^{\frac{3}{5}}$ and $x^{\frac{1}{4}}$ for $\alpha = 0$ and $\frac{1}{2}\pi$ respectively, where x is the streamwise distance from the leading edge, these different scalings then clearly imply the lack of similarity for intermediate values of α. The final point to note is that, again because of the different scalings, it may be expected that the dominance of the streamwise and normal components of the body force should depend not only on the inclination angle α but also on the streamwise distance x.

In view of the above considerations, we have developed a generalized formulation for the natural-convection boundary-layer flow over a flat plate of arbitrary inclination. The formulation identifies a proper set of boundary-layer variables through which the relative importance of the body force components can be assessed.

The formulation, analysis, and results are presented in the following.

2. Governing equations and preliminary considerations

We consider the two-dimensional, laminar, boundary-layer flow above an isothermal semi-infinite heated plate of temperature $T = T_w$ and inclination angle α. The otherwise stationary fluid has a temperature T_∞ and is Boussinesq. The flow configuration is shown in figure 1. The governing equations are

$$\frac{\partial u}{\partial x}+\frac{\partial v}{\partial y}=0, \tag{1}$$

$$u\frac{\partial u}{\partial x}+v\frac{\partial u}{\partial y}=-\frac{1}{\rho_\infty}\frac{\partial p}{\partial x}+\nu\frac{\partial^2 u}{\partial y^2}+g\beta(T-T_\infty)\sin\alpha, \tag{2}$$

$$0=-\frac{1}{\rho_\infty}\frac{\partial p}{\partial y}+g\beta(T-T_\infty)\cos\alpha, \tag{3}$$

$$u\frac{\partial T}{\partial x}+v\frac{\partial T}{\partial y}=\kappa\frac{\partial^2 T}{\partial y^2}, \tag{4}$$

subject to

$$u=v=0, \quad T=T_w \quad \text{at} \quad y=0, \tag{5}$$

$$u=0, \quad T=T_\infty \text{ outside the boundary layer.} \tag{6}$$

Here y is the distance normal to the plate, while u and v are the x and y velocity components. The kinematic viscosity, ν, thermal diffusivity, κ, and thermal expansion coefficient, β, are taken as constants for simplicity.

In order to gain further insight into the phenomenon, especially the different manner through which the normal and tangential components of buoyancy force drive the fluid along the plate, we integrate (3) to obtain

$$p=\rho_\infty g\beta(T_w-T_\infty)(\cos\alpha)\int_\infty^y \theta\,\mathrm{d}y, \tag{7}$$

which when substituted into (2) yields

$$u\frac{\partial u}{\partial x}+v\frac{\partial u}{\partial y}-\nu\frac{\partial^2 u}{\partial y^2}=g\beta(T_w-T_\infty)(\cos\alpha)\frac{\partial}{\partial x}\int_y^\infty \theta\,\mathrm{d}y+g\beta(T_w-T_\infty)(\sin\alpha)\,\theta, \tag{8}$$

where

$$\theta=\frac{T-T_\infty}{T_w-T_\infty}. \tag{9}$$

Evaluating (7) and (8) at the plate surface, $y = 0$, where the effects of both buoyancy force components become maximum, we obtain

$$p(x,y=0)=-\rho_\infty\beta(T_w-T_\infty)(\cos\alpha)\int_0^\infty \theta(x,y)\,\mathrm{d}y, \tag{10}$$

$$-\nu\frac{\partial^2 u}{\partial y^2}(x,y=0)=g\beta(T_w-T_\infty)(\cos\alpha)\frac{\partial}{\partial x}\int_0^\infty \theta(x,y)\,\mathrm{d}y+g\beta(T_w-T_\infty)(\sin\alpha). \tag{11}$$

The physical meaning of (10) and (11) is the following. First, (10) indicates that the normal buoyant force acting per unit distance of x induces a negative pressure at the plate surface. The magnitude of this pressure continuously increases downstream because of the monotonic increase of the thickness of the boundary layer, δ, which is proportional to the integral $\int_0^\infty \theta(x,y)\,\mathrm{d}y$ for near-unity-Prandtl-number fluids of interest. This therefore constitutes a streamwise pressure gradient force, $-\partial p/\partial x$, as represented by the first term on the right-hand side of (11). The second term there

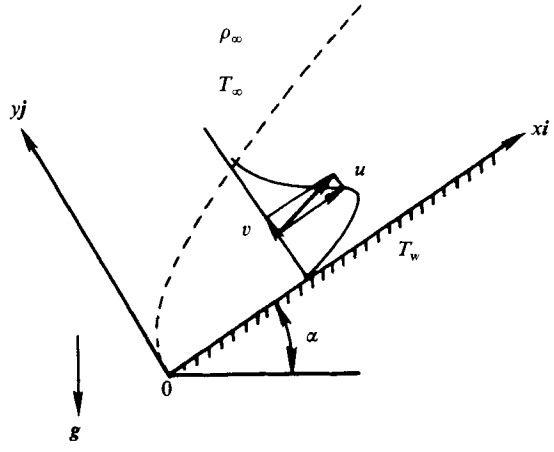

FIGURE 1. Configuration of the problem.

represents the streamwise buoyant force, which is a constant. Thus both components of the buoyant force contribute to the motion in the streamwise direction: indirectly through the normal component and directly through the tangential component. These two buoyant forces are balanced by the shear stress at the plate surface, given by the left-hand side of (11).

We further note that since the thermal boundary-layer thickness is expected to vary with $\delta \sim x^m$, where $\frac{1}{4} \leqslant m \leqslant \frac{2}{5}$, its derivative with x, $\mathrm{d}\delta/\mathrm{d}x$, diverges at the leading edge ($x = 0$) and decreases to zero as x tends to infinity. Since this term is represented by the normal buoyant force term in (11), and since the corresponding tangential buoyant force term is constant, we conclude that, as anticipated earlier based on scaling arguments, the tangential motion is dominated by the normal buoyant force near the leading edge and by the tangential buoyant force far downstream. The transition from the horizontal-plate-like flow to the vertical-plate-like flow is expected to take place at some streamwise distance x_t, which is determined by the inclination angle α and the strength of the buoyant force $g\beta(T_w - T_\infty)/\nu^2$.

Based on the above considerations, we now present a solution to this problem.

3. Analysis

We consider a dimensionless gauge function of x, $\hat{\xi}(x)$. Such a function can be constructed only through the local Grashof number

$$Gr = \frac{g\beta(T_w - T_\infty)\, x^3}{\nu^2}, \tag{12}$$

so that an appropriate choice of $\hat{\xi}(x)$ is

$$\hat{\xi} = Gr^{\frac{1}{4}}. \tag{13}$$

We normalize the y-coordinate by using the local boundary-layer thickness $\delta(x)$,

$$\eta = \frac{y}{\delta(x)} \tag{14}$$

with

$$\delta = \left[\frac{\nu^2}{g\beta(T_w - T_\infty)}\right]^{\frac{1}{4}} \hat{h}(\hat{\xi}). \tag{15}$$

Setting the streamfunction in the form

$$\psi = \nu G(\hat{\xi})\, F(\hat{\xi}, \eta), \tag{16}$$

(8) is transformed into

$$F''' - \left[\frac{\mathrm{d}G}{\mathrm{d}\hat{\xi}}\hat{h} - G\frac{\mathrm{d}\hat{h}}{\mathrm{d}\hat{\xi}}\right]F'^2 + \left[\frac{\mathrm{d}G}{\mathrm{d}\hat{\xi}}\right]\hat{h}FF'' - G\hat{h}\left[F'\frac{\partial F'}{\partial \hat{\xi}} - \frac{\partial F}{\partial \hat{\xi}}F''\right]$$
$$= -\frac{\hat{h}^3}{G}\left[\left\{\frac{\partial}{\partial \hat{\xi}}\left(\hat{h}\int_\eta^\infty \theta\,\mathrm{d}\eta\right) + \frac{\mathrm{d}\hat{h}}{\mathrm{d}\hat{\xi}}\eta\theta\right\}\cos\alpha + \theta\sin\alpha\right], \tag{17}$$

where prime designates differentiation with respect to η.

The above equations contain two arbitrary functions $\hat{h}$ and G. For their specification, we first require that our solution coincides with the similarity solutions for the limiting cases of $\alpha = 0$ and $\frac{1}{2}\pi$. This may be satisfied if we put

$$G = \frac{\hat{\xi}}{\hat{h}}. \tag{18}$$

Then, (17) becomes

$$F''' - \left[1 - 2\frac{\hat{\xi}}{\hat{h}}\frac{\mathrm{d}\hat{h}}{\mathrm{d}\hat{\xi}}\right]F'^2 + \left[1 - \frac{\hat{\xi}}{\hat{h}}\frac{\mathrm{d}\hat{h}}{\mathrm{d}\hat{\xi}}\right]FF'' - \hat{\xi}\left[F'\frac{\partial F'}{\partial \hat{\xi}} - \frac{\partial F}{\partial \hat{\xi}}F''\right]$$
$$= -\frac{\hat{h}^4}{\hat{\xi}}\left[\left\{\frac{\partial}{\partial \hat{\xi}}\left(\hat{h}\int_\eta^\infty \theta\,\mathrm{d}\eta\right) + \frac{\mathrm{d}\hat{h}}{\mathrm{d}\hat{\xi}}\eta\theta\right\}\cos\alpha + \theta\sin\alpha\right] \tag{19}$$

so that the coefficients of F'^2 and FF'' become constants for any $\hat{\xi}$-power of $\hat{h}$.

We may define $\hat{h}$ correctly to express the local thermal boundary-layer thickness, $\hat{\delta}_{\mathrm{T}}(\hat{\xi})$, in such a way that the non-dimensional temperature $\theta(\hat{\xi}, \eta)$ takes the value of 0.01, say, at a constant $\eta_\infty = \hat{\delta}_{\mathrm{T}}(\hat{\xi})/\hat{h}(\hat{\xi})$ for any $\hat{\xi}$. This condition, together with the other boundary conditions relevant, closes the problem and enables us to determine the functional form of $\hat{h}(\hat{\xi})$ simultaneously. But in this case we have to solve (19) with $\hat{h}$ unknown and there is no advantage over solving the original equation system. The difficulty in our problem lies in the point that different power dependences of the boundary-layer thickness at the two limiting cases make it difficult to obtain the solution which is uniformly valid over the whole domain. We would rather like to utilize the arbitrariness of the introduced function $\hat{h}$ to resolve this difficulty.

To specify the arbitrary function $\hat{h}(\hat{\xi})$, we require that such a specification should not alter the character of the equation in that changes in the flow variables, such as $\hat{h}(\hat{\xi})$ itself as well as the stream function F, should be of the order of unity in the $(\hat{\xi}, \eta)$-space. While there may exist a variety of ways to achieve this goal, the following physically-motivated specification appears to be quite adequate.

We consider (19) evaluated at $\eta = 0$:

$$-F'''(\hat{\xi}, 0) = \frac{\hat{h}^4}{\hat{\xi}}\left[\frac{\mathrm{d}}{\mathrm{d}\hat{\xi}}\left[\hat{h}\int_0^\infty \theta\,\mathrm{d}\eta\right]\cos\alpha + \sin\alpha\right], \tag{20}$$

where $F(\hat{\xi}, 0)$ and $F'(\hat{\xi}, 0)$ have been assumed zero as confirmed later. If $\hat{h}$ somehow represents the local boundary-layer thickness, then $F'''(\hat{\xi}, 0)$ and $\int_0^\infty \theta\,\mathrm{d}\eta$ should be quantities of $O(1)$ over the whole range of $\hat{\xi}$. For the case of $\alpha = 0$ the similarity solution assumes $\hat{h} = \hat{\xi}^{\frac{2}{5}}$ which yields $-F'''(\hat{\xi}, 0) = 0.692$ and $\int_0^\infty \theta\,\mathrm{d}\eta = 1.83$ while the other limiting case of $\alpha = \frac{1}{2}\pi$ with $\hat{h} = \hat{\xi}^{\frac{1}{3}}$ results in $-F'''(\hat{\xi}, 0) = 0.952$ and $\int_0^\infty \theta\,\mathrm{d}\eta = 1.85$. The very small differences between these two pairs of limiting values suggests

that both quantities have weak dependences on $\hat{\xi}$ and may be regarded as constants to specify $\hat{h}$. This assumption is similar to the idea involved in the Pohlhausen integral method, in which the functional form of F and θ in η are appropriately assigned as inputs. Hence, we write

$$B = \frac{\hat{h}^4}{\hat{\xi}}\left[A\frac{\mathrm{d}\hat{h}}{\mathrm{d}\hat{\xi}}\cos\alpha + \sin\alpha\right]. \tag{21}$$

This equation approximates (20) in an average sense, but is not equivalent to it. Therefore, we can use (21) as an additional independent equation in solving (19) even if $\hat{h}$ obtained from (21) does not correctly describe the change in the boundary-layer thickness. The advantage is to make it possible to find a solution to (20) which is uniformly valid over the whole range since (21), as shown in the Appendix, yields $\hat{h}$ with the correct power dependences in the limiting cases of $\alpha = 0$ and $\frac{1}{2}\pi$ to bridge them. Once the solution is obtained, it will be easy to reproduce the actual boundary-layer thickness from the solution.

We have not yet determined the values of A and B. Their choice is immaterial so far as they are constants of $O(1)$. The degree to which the resulting $\hat{h}$ approximates $\delta_{\mathrm{T}}(\hat{\xi})$, however, depends on the choice. This point may be checked by calculating $\eta_\infty(\hat{\xi})$. The better approximated $\hat{h}$ will yield less change in that value. An appropriate choice would be to use their mean values, but we may as well set one of them to be unity without loss of generality because the forms of (19) and the corresponding heat transfer equation are invariant in the transformation of $\hat{h}$, η and F to $C\hat{h}$, η/C and CF, where C is an arbitrary constant. Thus, (21) may be rewritten as

$$1 = \frac{\hat{h}^4}{\hat{\xi}}\left[K\frac{\mathrm{d}\hat{h}}{\mathrm{d}\hat{\xi}}\cos\alpha + \sin\alpha\right]. \tag{22}$$

We shall first put $K = 1$ and then proceed to find a best fitting value of K in order to show how the choice of K influences the degree of approximation of $\hat{h}$ to $\hat{\delta}_{\mathrm{T}}$. The influence of K is expected to weaken as $\alpha \to \frac{1}{2}\pi$, as shown in (22). Of course, the exact solution itself is in principle also not influenced by the choice of the K-value.

Thus together with the initial condition

$$\hat{h} = 0 \quad \text{at} \quad \hat{\xi} = 0, \tag{23}$$

the function $\hat{h}$ is defined.

Finally, the parameter α present in (19) and (22) can be eliminated through the transformations

$$\hat{\xi} = \frac{(\cos\alpha)^{\frac{4}{3}}}{(\sin\alpha)^{\frac{5}{3}}}\xi, \quad \hat{h} = \frac{(\cos\alpha)^{\frac{1}{3}}}{(\sin\alpha)^{\frac{2}{3}}}h. \tag{24}$$

Summarizing, the system of equations to be solved is the following.

Boundary-layer coordinates:

$$\xi = \left[Gr\,(x)\frac{\sin^5\alpha}{\cos^4\alpha}\right]^{\frac{1}{3}} \quad \text{with} \quad Gr = \frac{g\beta(T_{\mathrm{w}} - T_\infty)\,x^3}{\nu^2}, \tag{25}$$

$$\eta = \frac{y}{\delta(x)} \quad \text{with} \quad \delta = \left[\frac{\nu^2}{g\beta(T_{\mathrm{w}} - T_\infty)}\frac{\cos\alpha}{\sin^2\alpha}\right]^{\frac{1}{5}} h(\xi). \tag{26}$$

Flow variables:

$$\theta(\xi, \eta) = \frac{T - T_\infty}{T_{\mathrm{w}} - T_\infty}, \tag{27}$$

$$\psi = \nu\frac{\cos\alpha}{\sin\alpha}\frac{\xi}{h(\xi)}F(\xi, \eta). \tag{28}$$

Momentum equation:

$$F'''-\left[1-2\frac{\xi\,\mathrm{d}h}{h\,\mathrm{d}\xi}\right]F'^2+\left[1-\frac{\xi\,\mathrm{d}h}{h\,\mathrm{d}\xi}\right]FF''+\frac{h^4}{\xi}\left[\frac{\mathrm{d}h}{\mathrm{d}\xi}\int_\eta^\infty\theta\,\mathrm{d}\eta+\frac{\mathrm{d}h}{\mathrm{d}\xi}\eta\theta+\theta\right]$$
$$=\xi\left[F'\frac{\partial F'}{\partial\xi}-\frac{\partial F}{\partial\xi}F''-\frac{h^5}{\xi^2}\int_\eta^\infty\frac{\partial\theta}{\partial\xi}\mathrm{d}\eta\right]. \quad (29)$$

Energy equation:

$$\theta''+Pr\left[1-\frac{\xi\,\mathrm{d}h}{h\,\mathrm{d}\xi}\right]F\theta'=Pr\,\xi\left[F'\frac{\partial\theta}{\partial\xi}-\frac{\partial F}{\partial\xi}\theta'\right]. \quad (30)$$

Auxiliary equation (boundary-layer thickness):

$$\frac{h^4}{\xi}\left[K\frac{\mathrm{d}h}{\mathrm{d}\xi}+1\right]=1. \quad (31)$$

Boundary conditions:

$$F'(\xi,0)=0,\quad \left(1-\frac{\xi\,\mathrm{d}h}{h\,\mathrm{d}\xi}\right)F(\xi,0)=-\xi\frac{\partial F}{\partial\xi}(\xi,0),\quad \theta(\xi,0)=1, \quad (32)$$

$$F'(\xi,\infty)=0,\quad \theta(\xi,\infty)=0, \quad (33)$$

$$h(0)=0. \quad (34)$$

Solution of the problem can be further facilitated by replacing the second boundary condition in (32) by

$$F(\xi,0)=0. \quad (35)$$

In fact, integration of the original boundary condition yields

$$F(\xi,0)=C\exp\left[-\int\left(\frac{1}{\xi}-\frac{1}{h}\frac{\mathrm{d}h}{\mathrm{d}\xi}\right)\mathrm{d}\xi\right], \quad (36)$$

where C is the constant of integration. In the limit of $\xi\to 0$, we have $h\to\xi^{\frac{2}{5}}$ and

$$F(\xi,0)=C\xi^{-\frac{3}{5}}. \quad (37)$$

Since the similarity solution for the horizontal-plate case requires the vanishing of $F(0,0)$, the constant of integration, C, should be zero so that the present solution can match the similarity solution as ξ approaches zero. This establishes the use of (35).

The boundary-layer problem can be considered to be completely specified. There are two special solutions to this problem. From (25), $\alpha\to 0$ or $\frac{1}{2}\pi$ corresponds to $\xi\to 0$ or ∞ respectively. In these asymptotic limits the above partial differential equation system reduces to an ordinary differential equation system which governs the similarity solutions for the horizontal and vertical plate cases (see Appendix). Another special case of interest is the locally-similar solution defined by setting to zero all terms involving partial differentiation of F and θ with respect to ξ in the equation system.

4. Results and discussions

Both the exact solution and the locally-similar solution have been numerically obtained for an assumed Prandtl number of 0.72. Figure 2 shows the profiles of the function $\theta(\xi,\eta)$, calculated with $K=1$ in (31), in which the exact and locally-similar

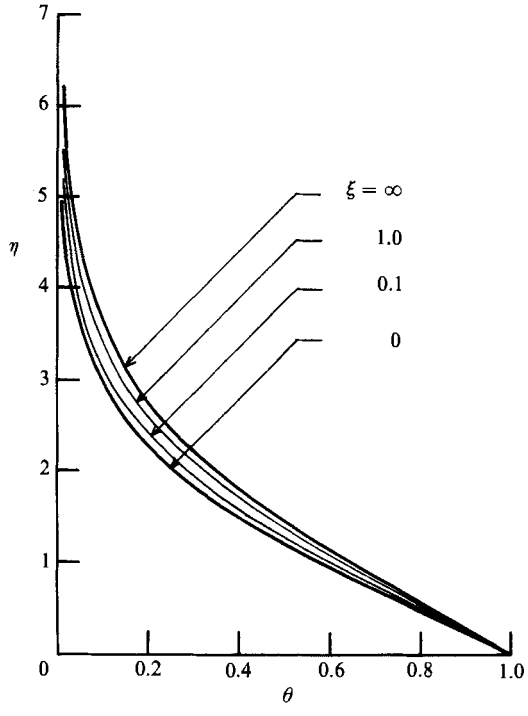

FIGURE 2. Exact and locally similar solutions of the temperature function $\theta(\xi, \eta)$ for $Pr = 0.72$, calculated on the basis of (31) with $K = 1$.

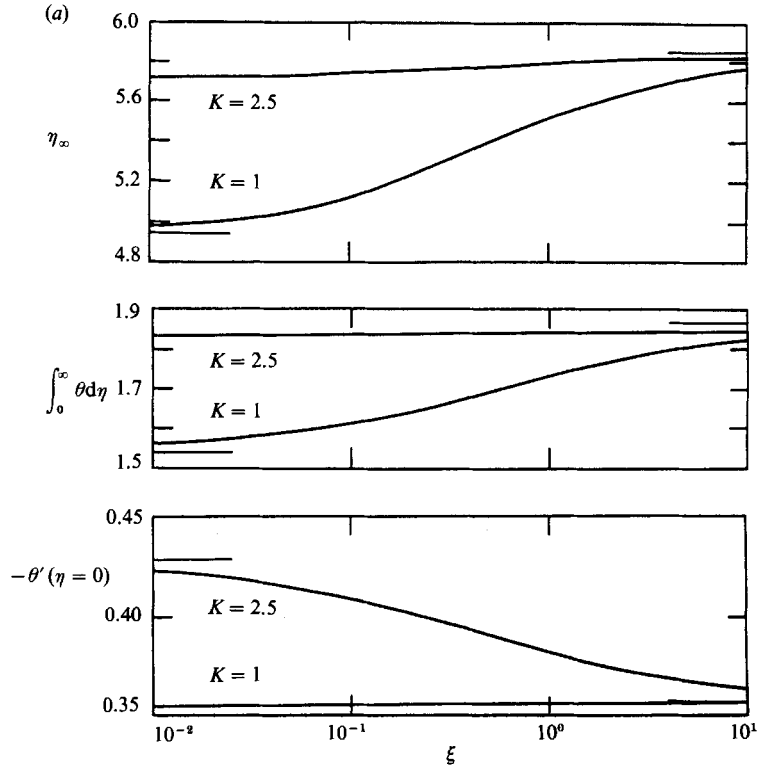

FIGURE 3(*a*). For caption see next page.

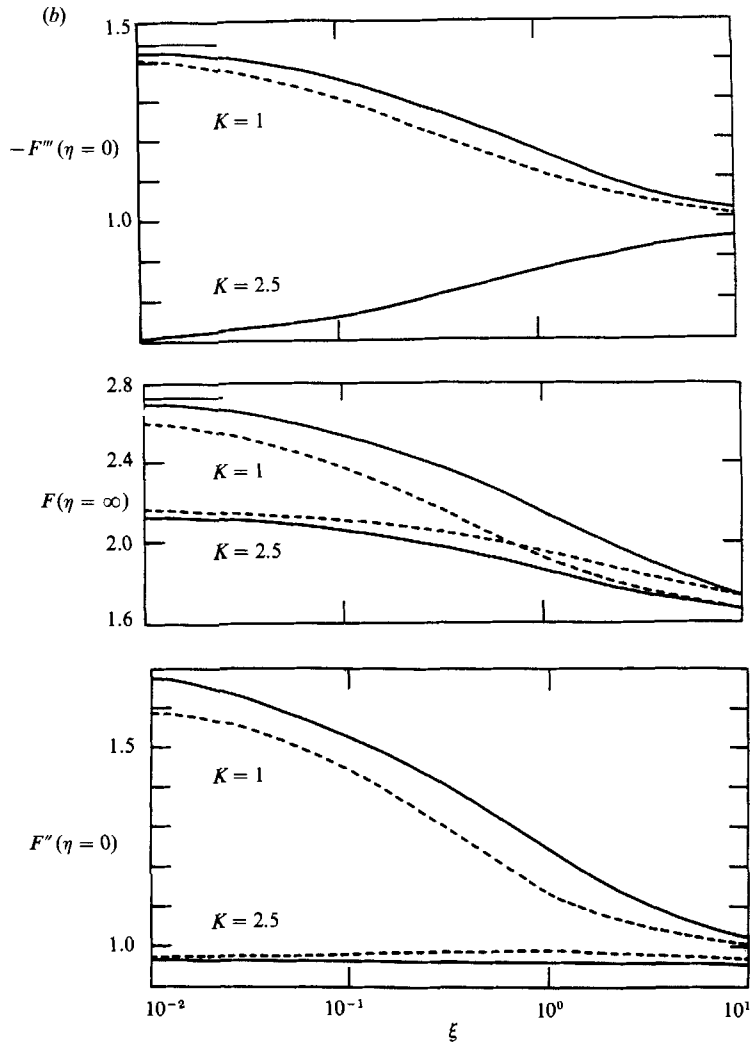

FIGURE 3. (*a*) Variations of characteristic thermal quantities with ξ. ——, exact solution; – – –, locally similar solution. (*b*) Variations of characteristic dynamic quantities with ξ. ——, exact solution; – – –, locally similar solution.

solutions are indistinguishable from each other. The local thermal boundary-layer thickness, $\delta_T(\xi)$, is derived by multiplying by $h(\xi)$ the value $\eta = \eta_\infty(\xi)$ at which the function $\theta(\xi, \eta)$ takes the value of 0.01. Figure 3(*a*) shows the variations of η_∞, $\int_0^\infty \theta \, d\eta$ and $\theta'(\xi, 0)$ with ξ. The exact and locally-similar solutions are again indistinguishable from each other, implying that the locally-similar solution is an adequate approximation of the thermal boundary layer.

Figure 4 shows the variation of h with ξ. In the figure the actual thermal boundary-layer thickness, δ_T, is also depicted in broken line for comparison. The solution shows a smooth transition from the horizontal to the vertical limits. The corresponding transition of m from $\frac{2}{5}$ to $\frac{1}{4}$ is shown in figure 5.

Figure 6 compares the velocity profiles of the exact solution with the locally similar solution. The adopted coordinates are normalized by use of the thermal boundary-layer thickness, so that one can see how the location of the maximum

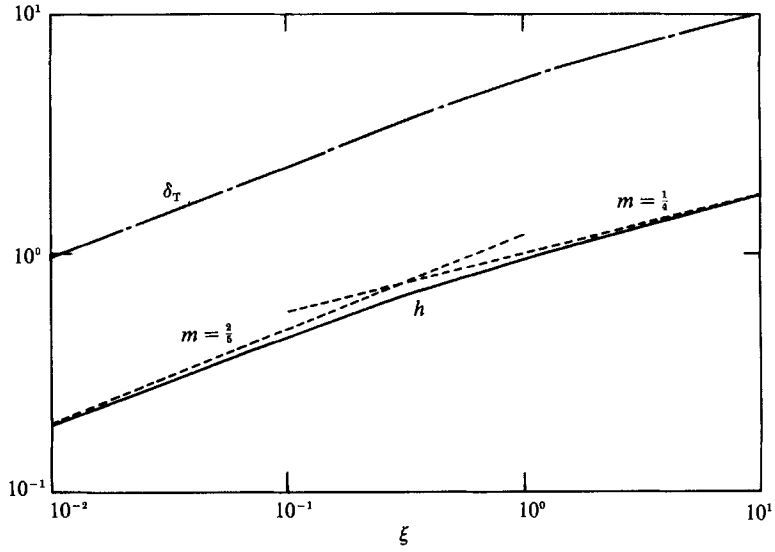

FIGURE 4. Variation of the boundary-layer-thickness function $h(\xi)$. In the limits of small and large ξ, h approaches the asymptotes $(\frac{5}{2})^{\frac{1}{5}}\xi^{\frac{2}{5}}$ and $\xi^{\frac{1}{4}}$, respectively, which are denoted by dashed lines. The intersection point of the asymptotes is $(\frac{2}{5})^{\frac{4}{5}} = 0.295$.

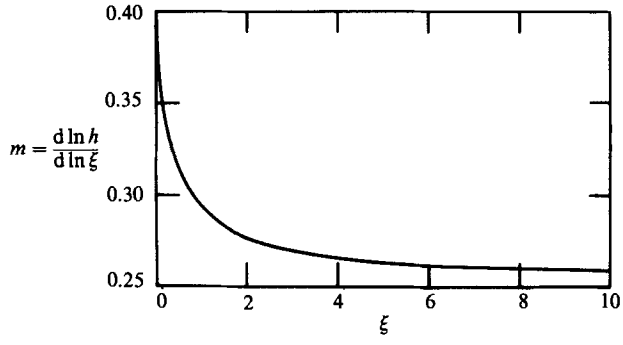

FIGURE 5. Variation of the exponent m between the horizontal-plate and vertical-plate limits.

velocity point changes within the thermal boundary layer. The figure indicates a gradual downward movement of the maximum velocity point in the course of transition from the horizontal-plate-like to the vertical-plate-like flow. Unlike the temperature profiles, the velocity profiles show substantial disagreement between the two solutions in the transition region.

The maximum deviation in $F(\xi, \infty)$, $F''(\xi, 0)$ and $F'''(\xi, 0)$ shown in figure 3(*b*) is about 10%. These results are consistent with the greater sensitivity of the velocity profiles to the buoyancy induced forces, thereby making it more sensitive to approximations in the analysis.

The functional form of h presented above is based on the auxiliary equation (31) with $K = 1$. Although the exact solution itself does not depend on the value of K, an appropriate choice of K-value gives the best fitting of h with δ_T in their form. The solutions for $K = 2.5$, shown in figure 3, appear to provide the best fit among several tested values. They show good uniformity over the whole range of ξ, and it was also found that, in this case, the temperature profiles in figure 2 degenerate to a single curve in a good approximation.

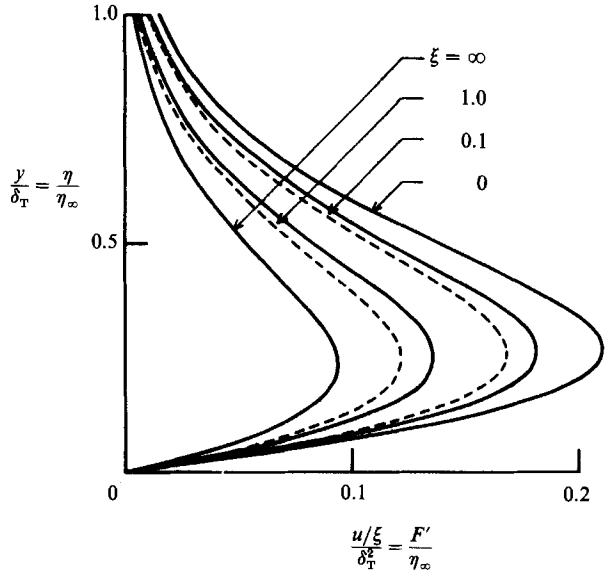

FIGURE 6. Exact and locally-similar solutions of the velocity function $F'(\xi, \eta)$ for $Pr = 0.72$. ——, exact solution; – – –, locally similar solution.

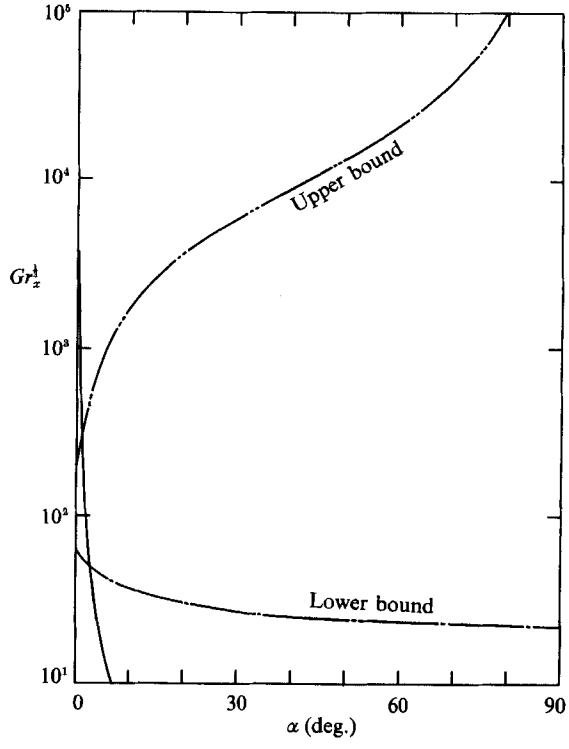

FIGURE 7. The transition Grashof number, Gr_t, as a function of the inclination angle α and upper and lower bounds on the boundary-layer approximation.

The transition distance x_t at which the flow pattern changes from being horizontal-plate-like to vertical-plate-like can be taken to be the x at which the magnitudes of the two buoyancy-force terms on the right-hand side of (11) become equal. The exact numerical solution gives $\xi_t = 0.341$, which is closely located at the intersection point of the two asymptotes in figure 4. The transition distance for a given inclination angle α is therefore given by

$$x_t = \xi_t \left[\frac{\nu^2}{g\beta(T_w - T_\infty)} \frac{\cos^4\alpha}{\sin^5\alpha}\right]^{\frac{1}{3}}. \tag{38}$$

Figure 7 shows the transition Grashof number, Gr_t, as a function of α. Above this line the vertical-plate-like flow pattern is dominant. The very small value of ξ_t in (38) makes the transition distance very small except near $\alpha = 0$ at which the factor $\cos^{\frac{4}{3}}\alpha/\sin^{\frac{5}{3}}\alpha$ becomes large. Thus the flow is vertical-plate-like over most of the plate length unless the inclination angle is very small. We also note that the transition point approaches the leading edge as the temperature difference, $(T_w - T_\infty)$, increases.

The quantities of engineering interest are the distributions of surface heat flux, Q, and shear stress, τ_w, along the plate. They are given in non-dimensional form by

$$\frac{\theta'(\xi, 0)}{h} = \left[\frac{\nu^2}{g\beta(T_w - T_\infty)} \frac{\cos\alpha}{\sin^2\alpha}\right]^{\frac{1}{3}} \frac{Q}{\lambda}, \tag{39}$$

$$\frac{F''(\xi, 0)}{h^3} = \left[\frac{\nu^2}{g\beta(T_w - T_\infty)} \frac{\cos\alpha}{\sin^2\alpha}\right]^{\frac{2}{3}} \frac{\tau_w}{\mu\nu}, \tag{40}$$

and can be evaluated from the values of $\theta'(\xi, 0)$, $F''(\xi, 0)$ and $h(\xi)$ in figures 3 and 4.

The results on the surface heat flux and shearing stress show that they have greater values near the leading edge for the horizontal plate than for the vertical plate. This is caused by the different fluid driving mechanisms in these two cases. That is, while the driving force along the plate is regular for the vertical plate, for the horizontal plate the driving force, $\partial p/\partial x$, diverges at $x = 0$, implying an impulsive force acting near the leading edge. As a result, near the leading edge the fluid flows faster for the horizontal plate than for the vertical plate, thereby resulting in a thinner boundary layer and greater surface heat flux and shearing stress.

The above behaviour, however, should be qualified on the validity of the boundary-layer assumption near the leading edge where the value of x becomes comparable with the local boundary-layer thickness. This lower limit in x for the boundary-layer assumption to hold can be estimated from the relation $x_L = \delta(x_L)$, which gives $x_L[g\beta(T_w - T_\infty)/\nu^2]^{\frac{1}{3}} = (\frac{5}{2})^{\frac{1}{15}}$ and 1 for $\alpha = 0$ and $\frac{1}{2}\pi$ respectively. These values are compared with the value of x at which the boundary-layer thicknesses for the $\alpha = 0$ and $\frac{1}{2}\pi$ cases become equal, given by $x_E[g\beta(T_w - T_\infty)/\nu^2]^{\frac{1}{3}} = (\frac{2}{5})^{\frac{4}{3}}$. Since $x_E < x_L$, the boundary-layer behaviour discussed in the previous paragraph is actually somewhat irrelevant. The dash-dot line near the bottom in figure 7 shows the lower bound on $Gr^{\frac{1}{3}}$ at various α when we employ $x_L(\xi) = 10h(\xi)$ as the limiting case. Below it the boundary-layer approximation is no longer valid.

There is also an upper limit to x. Since the temperature profile within the boundary layer has negative derivatives in the y-direction for $\alpha < \frac{1}{2}\pi$, the state is not dynamically stable. The increasing boundary-layer thickness along the plate makes the local Rayleigh number reach a critical value so that some kind of cellular convection is expected to take place at distances further downstream. Assuming that

the variation of the flow field in the x-direction is small compared with that in the y-direction, we may apply the stability analysis developed for the classical Bénard problem. The rigorous analysis, however, is not straightforward since the undisturbed state has a velocity field. Nevertheless, we may expect that this fact does not modify so much the values of the critical Rayleigh number which is obtained from the Bénard problem (Deardorff 1965). Thus, using the critical Rayleigh number for the fixed surface case, $Ra_c = 1100$, say, we may express our stability condition as

$$\Gamma(\xi)\, Ra_c > \frac{g\beta \cos\alpha (T_w - T_\infty)\, \delta^3}{\nu^2} = \frac{\cos^2\alpha}{\sin^2\alpha} h^3(\xi), \tag{41}$$

where Γ is a correction factor due to the difference of the problem. Since ξ is a function of the local Grashof number Gr and the inclination angle α, the above inequality predicts the position of occurrence of instability as a function of α. The calculated upper bound is shown in figure 7, assuming $\Gamma = 1$. The same figure indicates that the transition is observed only at small α in the range of validity of the boundary-layer approximation.

In particular for $\alpha = 0$ the critical Rayleigh number is determined from the value of the critical Gr, consistent with the experimental result by Rotem & Claassen (1969). Of course, such an instability does not occur for the case of $\alpha = \frac{1}{2}\pi$. Once the instability condition is met, the boundary layer may grow rapidly because, in our problem, the outer edge of the boundary layer is not restricted by any constraint. This situation is similar to what is observed in the horizontal thermal boundary layers of the fixed surface convection cell. In this case the instability leads to the separation into smaller cells.

5. Concluding remarks

In the present study we have successfully obtained a generalized formulation for the natural convection boundary-layer flow over a heated plate with arbitrary inclination. The formulation reveals the important physical insight that the flow characteristics depend not only on the extent of inclination but also on the distance from the leading edge. Thus, except for the limiting cases of $\alpha = 0$ and $\frac{1}{2}\pi$, the flow is horizontal-plate-like near the leading edge and is vertical-plate-like downstream of it. Furthermore, the driving force for the flow has an impulsive character near the leading edge but becomes more regular further downstream.

It is also of interest to note the close agreement between the exact and locally-similar solutions. This is reasonable because the general solution is bounded by two similarity solutions, and because the boundary conditions remain the same for all inclinations. The availability of an accurate locally-similar solution, and the existence of such a locally-similar flow as implicated by it, are expected to facilitate future theoretical and experimental developments.

Dr S. Nam assisted in obtaining the numerical solution of an earlier version of the formulation. This research was supported by the Heat Transfer Program of the US National Science Foundation. A. Umemura was on leave from Yamagata University, Japan.

Appendix

Here we present the self-similar as well as the perturbed equations for $\alpha = 0$ and $\frac{1}{2}\pi$ from the generalized formulation.

Recognizing that the right-hand side of (29) and (30) vanish at $\xi = 0$ and ∞, let us first consider their asymptotic form as $\xi \to 0$. Here, in order to satisfy $h = 0$ at $\xi = 0$, we assume $h \sim \xi^n$, $n > 0$. It can then be shown that this function has the property that as $\xi \to 0$, both $dh/d\xi$ and ξ^2/h^8 diverge and $1 > n > 0$. Using this property in (31) readily yields

$$\frac{dh}{d\xi} = \frac{1}{K}\frac{\xi}{h^4}, \tag{A 1}$$

which upon integration yields

$$h = \left(\frac{5}{2K}\right)^{\frac{1}{5}} \xi^{\frac{2}{5}}. \tag{A 2}$$

Substituting (A 2) into (15) gives the boundary-layer thickness

$$\delta = \left[\frac{5}{2K}\frac{\nu^2}{g\beta(T_w - T_\infty)}\right]^{\frac{1}{5}} x^{\frac{2}{5}} \quad \text{for} \quad \alpha = 0. \tag{A 3}$$

Furthermore, (A 3) reduces (29) and (30) to

$$F''' - \tfrac{1}{5}F'^2 + \tfrac{3}{5}FF'' + \int_\eta^\infty \theta \, d\eta - \eta\theta = 0, \tag{A 4}$$

$$\theta'' + \tfrac{3}{5}Pr\, F\theta' = 0, \tag{A 5}$$

which are the self-similar equations for the horizontal-plate case.

In the limit of $\xi \to \infty$, if $dh/d\xi$ is finite or divergent, then $h \sim \xi^{1+n}, n \geqslant 0$, which results in $\xi^2/h^8 \to 0$ and hence an imaginary value for $dh/d\xi$. This contradicts the original assumption, implying that $dh/d\xi \to 0$ as $\xi \to \infty$ in (31). Consequently

$$h = \xi^{\frac{1}{4}} \tag{A 6}$$

which yields

$$\delta = \left[\frac{\nu^2}{g\beta(T_w - T_\infty)}\right]^{\frac{1}{4}} x^{\frac{1}{4}} \quad \text{for } \alpha = \tfrac{1}{2}\pi, \tag{A 7}$$

and casts (29) and (30) into the self-similar form for the vertical case,

$$F''' - \tfrac{1}{2}F'^2 + \tfrac{3}{4}FF'' + \theta = 0, \tag{A 8}$$

$$\theta'' + \tfrac{3}{4}Pr\, F\theta' = 0. \tag{A 9}$$

Starting with the above self-similar solution, the perturbation solution from the horizontal-plate case is obtained as follows. For small ξ we may regard $f \ll 1$ for $h = (5/2K)^{\frac{1}{5}}\xi^{\frac{2}{5}}(1+f)$, and (31) may be linearized to

$$\tfrac{3}{2}z\frac{df}{dz} + \left(\frac{5}{2K}\right)^{\frac{4}{5}} z = \frac{1}{(1+f)^4} - (1+f) \approx -5f \quad \text{with } z = \xi^{\frac{3}{5}}, \tag{A 10}$$

which has the general solution

$$f = -\frac{10}{13}\left(\frac{5}{2K}\right)^{\frac{4}{5}} \xi^{\frac{3}{5}} + C\xi^{-2}. \tag{A 11}$$

Here the constant of integration, C, must be zero because of the condition $f(0) = 0$. Thus, it is expected that F and θ as well as f are expanded about $\xi = 0$ in power series of $\xi^{\frac{3}{5}}$. The first terms F_1 and θ_1 obey

$$F_1''' = F_0' F_1' + \tfrac{3}{5} F_0 F_1'' + \tfrac{6}{5} F_0'' F_1 + \frac{1}{2K}\int_\eta^\infty \theta_1 \,\mathrm{d}\eta + \frac{1}{K}\eta\theta_1$$

$$= \left(\frac{5}{2K}\right)^{\frac{4}{5}}\left[-\tfrac{6}{13} F_0 F_0'' + \tfrac{12}{13} F_0'^2 - \theta_0 + \frac{5}{K}\left(\int_\eta^\infty \theta_0 \,\mathrm{d}\eta + \eta\theta_0\right)\right] \quad \text{(A 12)}$$

$$\theta_1'' + Pr[\tfrac{3}{5} F_0 \theta_1' - \tfrac{3}{5} F_0' \theta_1 + \tfrac{6}{5}\theta_0' F_1] = -Pr\frac{6}{13}\left(\frac{5}{2K}\right)^{\frac{4}{5}} F_0 \theta_0', \quad \text{(A 13)}$$

subject to

$$F_1(0) = F_1'(0) = F_1'(\infty) = \theta_1(0) = \theta_1(\infty) = 0. \quad \text{(A 14)}$$

where F_0 and θ_0 are given by the solutions to (A 4) and (A 5).

Similarly for large ξ we put $h = \xi^{\frac{1}{4}}(1+f)$. The linearized equation for small f gives the general solution

$$f = -\tfrac{1}{3}\xi^{-\frac{1}{4}} \exp(-\tfrac{16}{3}\xi^{\frac{3}{4}})\left[\int \xi^{\frac{3}{4}} \xi'^{-\frac{2}{3}} \exp(\tfrac{16}{3}\xi')\,\mathrm{d}\xi' + C\right]. \quad \text{(A 15)}$$

It should be noted that this solution vanishes for any finite value of C as ξ tends to infinity. In fact, it is this integration constant that makes the solution connect to the other limiting solution above. The functions F and θ therefore cannot be expanded in a regular expansion form, for example as a power series in $\xi^{-\frac{3}{4}}$, unlike the perturbation solution from the horizontal-plate case.

REFERENCES

Deardorff, J. W. 1965 Gravitational instability between horizontal plates with shear. *J. Fluid Mech.* **8**, 1027–1030.

Gill, W. N., Zeh, D. W. & Del-Casel, E. 1965 Free convection on a horizontal plate. *Z. angew. Math. Phys.* **16**, 532–541.

Ostrach, S. 1953 An analysis of laminar free-convection flow and heat transfer about a flat plate parallel to the direction of the generating body force. *NACA Tech. Rep.* 1111.

Rotem, Z. & Claassen, L. 1969 Natural convection above unconfined horizontal surfaces. *J. Fluid Mech.* **38**, 173–192.

Stewartson, K. 1958 On free convection from a horizontal plate. *Z. angew. Math. Phys.* **9***a*, 276–282.